PROCEEDINGS OF SPIE

SPIEDigitalLibrary.org/conference-proceedings-of-spie

Sensorless adaptive optics with a laser free spinning disk confocal microscope

Hussain, S. A., Kubo, T., Hall, N., Hampson, K., Phillips, M., et al.

S. A. Hussain, T. Kubo, N. Hall, K. Hampson, M. A. Phillips, D. Gala, I. M. Dobbie, J. Antonello, M. Wincott, I. Davis, M. J. Booth, "Sensorless adaptive optics with a laser free spinning disk confocal microscope," Proc. SPIE 11248, Adaptive Optics and Wavefront Control for Biological Systems VI, 112480W (17 February 2020); doi: 10.1117/12.2542959

SPIE.

Event: SPIE BiOS, 2020, San Francisco, California, United States

Sensorless adaptive optics with a laser free spinning disk confocal microscope

S. A. Hussain[1]*, T. Kubo[2], N. Hall[3], K. Hampson[1], M. A. Phillips[3], D. Gala[3], I. M. Dobbie[3], J. Antonello[1], M. Wincott[1], I. Davis[3] and M. J. Booth[1]
[1] Department of Engineering Science, University of Oxford, Parks Road, Oxford OX1 3PJ, UK
[2] Department of Applied Physics, Osaka University, Osaka 565-0871, Japan
[3] Micron Advanced Bioimaging Unit, Department of Biochemistry, University of Oxford, South Parks Road, Oxford OX1 3QU, UK
*syed.hussain@eng.ox.ac.uk

ABSTRACT

Specimen induced aberrations can have detrimental effects in all types of high-resolution microscope. In this study, we present a sensorless technique that uses a deformable mirror (DM) to correct aberrations of both the system and sample. Using a laser-free confocal microscope, with patterned disk illumination and detection. The system is based on a commercial confocal module (Clarity, Aurox Ltd., UK) that uses Light Emitting Diode (LED) illumination to obtain optically sectioned 3D images. The results obtained show that the setup was able to correct aberrations of biological samples used in the study. These systems will help researchers working on various biological systems to obtain improved quality images when focussing deep into thick specimens.

1. INTRODUCTION

Microscopes provide powerful tools to scientists to observe various biological mechanism in different types of samples. This has helped reveal information about samples and resulted in numerous significant scientific discoveries[1–3]. Although it is relatively easy to image the sample at the interface, it becomes much more difficult to image at depth inside the tissue as differences in refractive indices and the existence of other biological structures give rise to unavoidable aberrations, which represent a departure of wavefront from its ideal shape. To overcome this difficulty, adaptive optics can be used in conjunction with the microscope to correct the wavefront and improve image quality. Components like Deformable Mirrors (DMs) and Spatial Light Modulators (SLMs) can be used for this purpose. With a DM this is achieved by using a thin membrane whose shape is modulated to compensate for the aberrations in the wavefront. This shape is changed by a network of actuators behind the membrane alter its shape. Alternatively, a lquid crystal SLM has small pixels whose refractive indices are changed to provide the same effect. These devices provide a wavefront distortion that is equal and opposite to that present in the system and specimen. The resulting aberration free images permit improved visualisation of fine details of the sample.

Confocal microscopes have played a major role in the study of various biological systems, particularly when imaging is required deep inside the specimen[4]. The main principle of this type of microscope is to eliminate the light from regions that are out of focus and allow only the light from the focal plane to reach the detector, usually a photomultiplier tube or other photodetector. By combining this microscope with AO techniques, important fine details of the specimens could be observed at depths that were not possible before[5].

In order to correct for the optical aberrations, we must first know the aberrations present. There are two principal methods to doing this. The first is Direct Wavefront Sensing (DWS), using devices such as interferometers or a Shack-Hartmann wavefront sensor to infer from intensity measurements the wavefront phase[6]. The deviation of the wavefront phase from the ideal flat wavefront determines the amount of aberration present that needs to be corrected. However, this aberration detection method is useful in a limited number of applications in fluorescence microscopy, since the extended 3D nature of biological samples can make such sensor readings ambiguous[7]. This method has however been successfully applied in multiphoton microscopes. More commonly, for detecting sample-induced aberrations, we rely on Sensorless Adaptive Optics (SAO) methods[8–10]. The principle underpinning SAO methods is broadly the same. Some property associated with a “good image” (e.g. contrast, spatial frequency power, second moment of the image Fourier transform, etc) is chosen as an image quality metric. Various amounts of different aberrations are applied, and the image quality

Adaptive Optics and Wavefront Control for Biological Systems VI, edited by Thomas G. Bifano, Sylvain Gigan, Na Ji, Proc. of SPIE Vol. 11248, 112480W · © 2020 SPIE · CCC code: 1605-7422/20/$21 · doi: 10.1117/12.2542959

metric is iteratively maximised for each one. In this scheme, different aberrations are corrected for sequentially whereas with DWS it is possible to correct for all the aberrations present at once. However, SAO can be used to correct for sample induced aberrations and requires no additional hardware beyond that already present in any imaging system.

In this study we present the potential of our system by using FluoCells' Bovine Pulmonary Artery Endothelial (BPAE) cells and *Drosophila melanogaster* larval neuromuscular junction (NMJ) - muscles 6&7, segment 3.

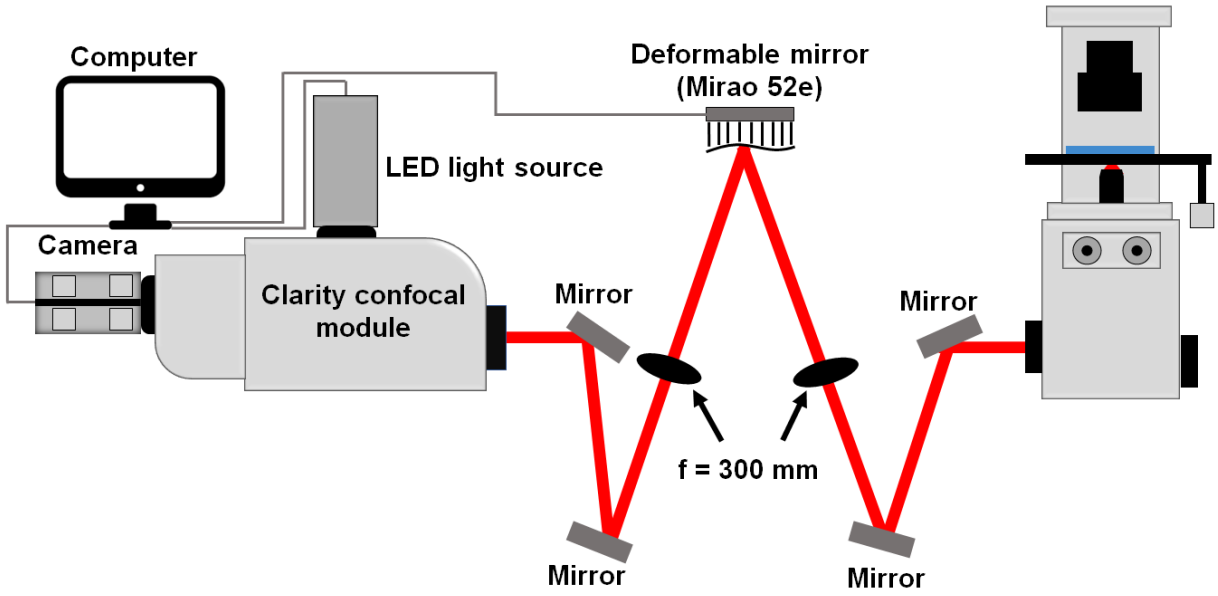

Fig 1. Experimental set-up used in the study. The experimental set-up consists of the Aurox Clarity confocal microscope module and Olympus IX71 inverted microscope. Other components are DM (Mirao 52 e), Mirrors and two f=300 mm lenses that reimage the output image from the microscope side port via the deformable mirror onto the input port of the Clarity module.

2. METHODS AND MATERIALS

Experimental setup: In this study, we used a commercial confocal microscope unit (Model: Clarity, Manufacturer: Aurox Ltd., United Kingdom) that used an array of LEDs along with a rotating disk that introduces both structured illumination and structured filtering of the imaged fluorescence. The unit is capable to provide images that are similar to confocal images with optical sectioning by using the structured illumination and detection technique. This is distinct from a traditional confocal microscope that uses laser illumination in a point scanning method.

Based on the fluorescence channel under investigation, the light that comes from the LED source is filtered by using an appropriate excitation filter. Patterned illumination is achieved by using a disk that that has a binary pattern on it. The dark lines on the disk reflect the light back whereas the transparent region allows the light to pass through the disk. When the incident light falls on the disk, half of the intensity passes through it and half of the light is reflected backwards and lost. This transmitted light is focused into the sample and generates fluorescence emission light that is imaged back onto the disk. The disk is at the conjugate image plane and the returned light consists of both in focus and out of focus components a combination of a wide field (WF) image and a confocal-like (C) image. At the disk the light that is transmitted has half of the intensity of C and WF, $0.5\times(WF + C)$, whereas the reflected light from the reflective part of the disk provides half intensity of WF and does not have intensity contribution due to confocal image, $0.5\times(WF - C)$. Both transmitted and reflected images are captured side-by-side on a single camera. By using image processing, we can subtract both images to obtain a confocal image. The disk also rotates at a high speed, much faster than the camera

exposure time to ensure that the structure of the illumination pattern is averaged out and the whole of the field of view is evenly sampled.

In normal operation, the Clarity module would be attached directly to the microscope body. For these experiments, we created an intermediate pupil plane to insert a DM (Imagine Optic, Mirao, 52e), Fig. 1. The DM is sited in the middle of a telescope made from two f=300 mm achromatic doublet (Thorlabs, United States) lenses that provide a conjugate pupil plane for the DM. The optical arrangement of this system was confirmed by using numerical simulation in Zemax (Zemax, United Kingdom). To test the setup we used biological samples and a 60x (NA=1.4) oil immersion microscope objective (Olympus, Japan). Broadband dielectric mirrors (Thorlabs, see Fig 1) were used to steer the beam between the Clarity, DM and microscope side port.

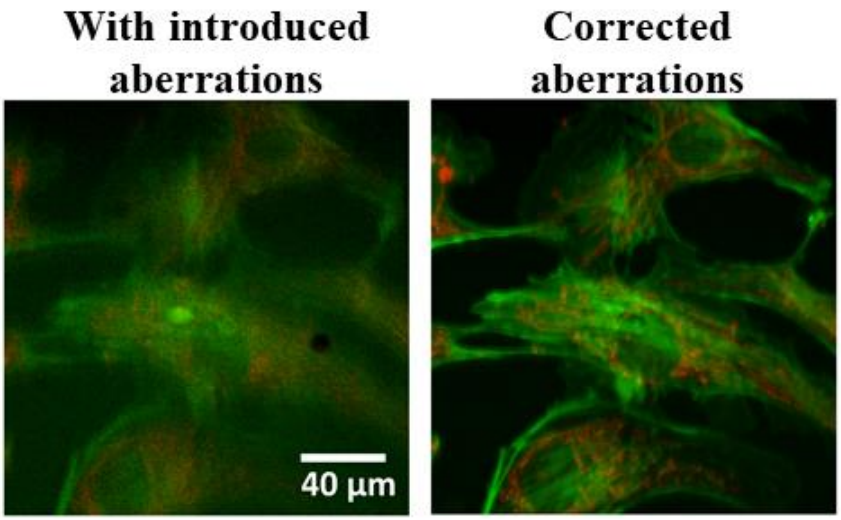

Fig. 2 Fluorescent images of the BPAE cells. MitoTracker™ CMXRos is presented in red whereas Alexa Fluor™ Phalloidinin green.

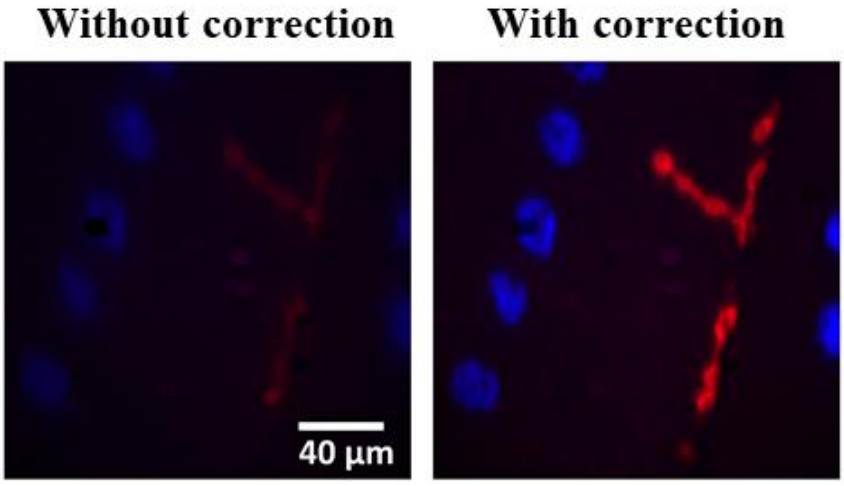

Fig. 3 Fluorescent images obtained in the NMJ. Nuclei (DAPI) are labelled in blue and the synapse (DLG, Alexa Fluor™) in red.

Sensorless AO: The SAO method follows a similar process as has already been described[11–13]. For each aberration being corrected, a number of images are taken and an image quality metric is determined. These image quality metric values

are used to fit a parabola and the peak of this parabola is taken to be the optimal correction for the current mode. This method is implemented in AOtools, an extension to Python Microscope[14]. AOtools has a suite of image quality metrics available, including the Second Moment of the Fourier Transform and Contrast.

3. RESULTS AND CONCLUSION

Figure 2 presents the results that we obtained when we used BPAE cells. In this case, we first intentionally introduced aberration in the experiment by using the DM and corrected this and other aberrations of the (OSA Zernike 3, 5 and 12, which are oblique astigmatism, vertical astigmatism and primary spherical modes) by using a sensorless algorithm. In this picture we can see two channels. The red channel represents MitoTracker™ CMXRos whereas green is Alexa Fluor™ Phalloidin. Comparing the two pictures with the induced aberrations and removal of these aberrations plus any additional aberrations due to optical setup, we can see the corrected image has better focus and fine details become more visible thatn in the uncorrected image. We later used NMJ samples, Fig. 3. In this case we had not introduced any aberration but used the system to correct sample-induced and system aberrations. In this picture, blue represents Nuclei (DAPI) and red shows Synapse (DLG, Alexa Fluor™). Comparing the two pictures in this case, the picture with AO correction has better contrast and reveals fine details. Moreover, synapses (in red) that were barely visible in the uncorrected image become visible in the corrected image.

In conclusion, we have corrected aberrations of both the system and the sample using the sensorless technique. The acquired images were able to show details that were not possible to obtain when not using AO.

4. DECLARATION

One of the authors (MJB) declares a significant interest in Aurox Ltd.

5. ACKNOWLEDGMENT

This research was funded by the Wellcome trust Strategic Award 107457, PI Prof. Ilan Davis. Nicholas Hall is supported by funding from the Engineering and Physical Sciences Research Council (EPSRC) and Medical Research Council (MRC) (grant number EP/L016052/1). European Research Council (ERC) under the Horizon 2020 research and innovation program (AdOMiS, grant agreement No. 695140)

6. REFERENCES

[1] Wollman, R., and Stuurman, N., "High throughput microscopy: from raw images to discoveries," Journal of Cell Science 120(21), 3715–3722 (2007).

[2] Lee, E.H., Hsin, J., Sotomayor, M., Comellas, G., and Schulten, K., "Discovery Through the Computational Microscope," Structure 17(10), 1295–1306 (2009).

[3] Shi, C., Luu, D.K., Yang, Q., Liu, J., Chen, J., Ru, C., Xie, S., Luo, J., Ge, J., et al., "Recent advances in nanorobotic manipulation inside scanning electron microscopes," Microsystems & Nanoengineering 2(1), 16024 (2016).

[4] Nwaneshiudu, A., Kuschal, C., Sakamoto, F.H., Rox Anderson, R., Schwarzenberger, K., and Young, R.C., "Introduction to Confocal Microscopy," Journal of Investigative Dermatology 132(12), 1–5 (2012).

[5] Tao, X., Fernandez, B., Azucena, O., Fu, M., Garcia, D., Zuo, Y., Chen, D.C., and Kubby, J., "Adaptive optics confocal microscopy using direct wavefront sensing," Optics Letters 36(7), 1062 (2011).

[6] Booth, M.J., "Adaptive optical microscopy: the ongoing quest for a perfect image," Light: Science & Applications 3(4), e165–e165 (2014).

[7] Rahman, S.A., and Booth, M.J., "Direct wavefront sensing in adaptive optical microscopy using backscattered light," Applied Optics 52(22), 5523 (2013).

[8] Žurauskas, M., Barnstedt, O., Frade-Rodriguez, M., Waddell, S., and Booth, M.J., "Rapid adaptive remote focusing microscope for sensing of volumetric neural activity," Biomedical Optics Express 8(10), 4369 (2017).

[9] Linhai, H., and Rao, C., "Wavefront sensorless adaptive optics: a general model-based approach," Optics Express 19(1), 371 (2011).

[10] Song, H., Fraanje, R., Schitter, G., Kroese, H., Vdovin, G., and Verhaegen, M., "Model-based aberration correction in a closed-loop wavefront-sensor-less adaptive optics system," Optics Express 18(23), 24070 (2010).

[11] Hofer, H., Sredar, N., Queener, H., Li, C., and Porter, J., "Wavefront sensorless adaptive optics ophthalmoscopy

in the human eye," Optics Express 19(15), 14160 (2011).
[12] Jian, Y., Xu, J., Gradowski, M.A., Bonora, S., Zawadzki, R.J., and Sarunic, M. V., "Wavefront sensorless adaptive optics optical coherence tomography for in vivo retinal imaging in mice," Biomedical Optics Express 5(2), 547 (2014).
[13] Booth, M.J., "Wavefront sensorless adaptive optics for large aberrations," Optics Letters 32(1), 5 (2007).
[14] "https://github.com/MicronOxford/microscope."